A comparison of different alignment approaches for the segmented grazing incidence mirrors on Constellation-X

Paul B. Reid[a†], David Caldwell[a], William Davis[a], Mark Freeman[a], Scott Owens Rohrbach[b], William Podgorski[a], and William Zhang[b]
[a] Harvard-Smithsonian Center for Astrophysics, 60 Garden St., Cambridge MA 02138
[b] NASA Goddard Space Flight Center, Greenbelt MD 02177

ABSTRACT

Each of the four Spectroscopy X-ray Telescopes (SXT) on Constellation-X contain a mirror assembly comprised of 2600 primary and secondary mirror segments. Critical to the performance of the mirror assemblies is the alignment of secondary to primary, and alignment of mirror pairs to one another. Focus errors must be corrected in order to meet imaging error budgets. The use of segmented mirrors enables unique alignment strategies not feasible with mirror shells of a full revolution. We discuss the relative advantages and disadvantages of two Con-X alignment strategies to minimize focus errors between shells. In the first approach, the mirrors are bent azimuthally to adjust the focal length of the mirror pair. In the second approach, coma is used to compensate for the transverse focus error. We examine the limits of applicability of the two approaches, and also discuss alignment error budgets.

Keywords: x-ray optics, alignment, focus correction, Constellation-X, Con-X

1. INTRODUCTION

Constellation-X (Con-X) is the next large x-ray observatory-class mission planned by NASA. In the 2000-2010 Decadal Survey it was ranked second in priority for large missions, behind the James Webb Space Telescope. Con-X will be used to study a wide range of astrophysical phenomena, focusing on a number of fundamental questions; (1) how do black holes grow and evolve, and are they the objects predicted by General Relativity, (2) when and how did the largest structures in the Universe form and evolve, and (3) what are the lifecycles of mater and energy.

To achieve these goals, the Con-X Spectroscopy X-ray Telescope (SXT) requires a bandwidth of 0.25 to 12 keV, with an effective area exceeding 1.5 m^2 at 1.25 keV and 0.6 m^2 at 6 keV. The Con-X mission and SXT have been described in references 1-2. To reduce mission cost and complexity, Con-X has been re-scoped several times. Currently, the mission consists of a single spacecraft launched on an Atlas V 551 vehicle. This spacecraft will contain four 1.32 meter diameter SXTs mounted to a common metering structure with a 10 m focal length, as shown in Figure 1. This architecture is described in reference 3. Alternative designs with a single mirror assembly as large as 3.4 m diameter and with a 20 m focal length are also being considered. These designs include an extensible optical bench and are still suitable for an Atlas V launch vehicle.

All the Con-X mirror designs consist of a Wolter I telescope, with segmented, thermally formed mirrors (see references 3-4). The use of thin, thermally formed, mirrors enables dense nesting of mirror shells with very high area to mass, and relatively low cost production. An image of the flight mirror assembly, showing its modular design which contains segmented optics, is shown in figure 2.

† email: preid@cfa.harvard.edu, phone: 1-617-495-7233, fax: 1-617-495-7356

Space Telescopes and Instrumentation 2008: Ultraviolet to Gamma Ray, edited by Martin J. L. Turner, Kathryn A. Flanagan, Proc. of SPIE Vol. 7011, 701111, (2008) · 0277-786X/08/$18 · doi: 10.1117/12.789658

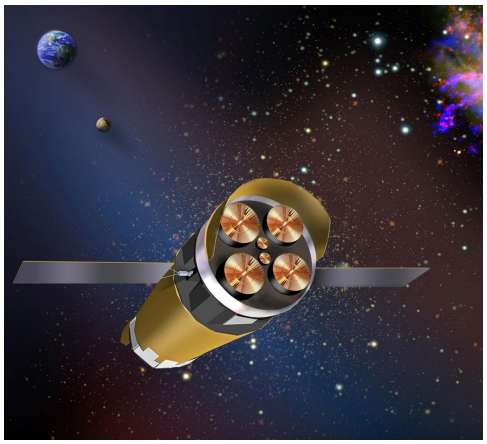

Figure 1: Artists conception of the 4 SXT version of Con-X

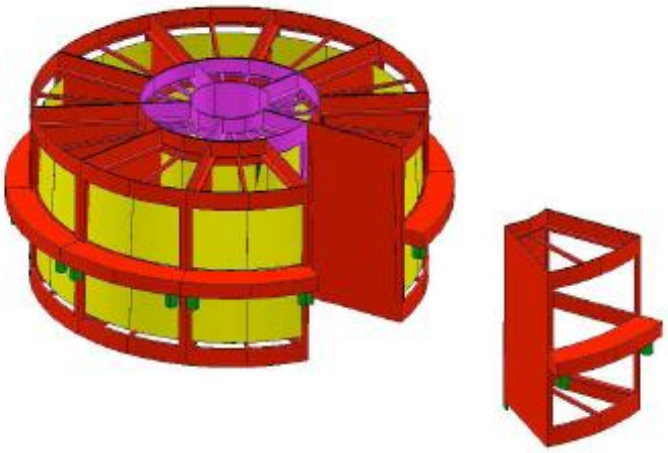

Figure 2: Segmented structure of a Con-X mirror assembly. In this figure the optical axis of the mirror assembly is vertical. Mirror segments are placed in either the red or purple modules, depending upon their radius.

To achieve imaging resolution performance requirements and goals, the primary and secondary mirror segments (or just 'segments') must all be aligned to be confocal. Focus errors between segment pairs and shells can result from errors in the thermal forming mandrels, be introduced during the thermal forming process, or during the support and mounting of the mirror segments. Segmented, thin mirrors allow different alignment degrees of freedom when compared to full shell, stiffer, mirrors such as on Chandra or XMM Newton. In particular, correction of focus errors is amenable to two different alignment approaches. In this paper we describe these two competing alignment approaches for thin segmented Wolter I mirrors, and discuss their relative advantages and limitations.

2. ALIGNMENT APPROACHES

Three major alignment aberrations must be minimized to successfully align the mirror segments. First,

the many shells must have their optical axes co-aligned, i.e., relative tilt is removed. As the primary and secondary mirror pair are functionally equivalent to a thin lens, this requires the primary mirrors to all have their optical axes co-aligned. Second, all the mirror segment primary-secondary (P-S) pairs must have a common focus. And lastly, we desire a minimal amount of coma, which implies that the secondary mirrors are aligned to their corresponding primary mirrors in tilts and decenter.

The use of segmented mirrors brings alignment advantages and disadvantages relative to full shell Wolter I telescopes. One disadvantage for segmented mirrors is that relative to a full shell design, many more alignments are required because there are several primary and secondary segments per shell. However, there are two advantages to segmented mirror alignment that are important. In the event of a manufacturing error in the focal length, one advantage is that flexible mirrors can have their focal length adjusted by deforming the mirrors so as to change their cone angles. A second advantage is that focus can be compensated to a degree by balancing it with coma. Neither of these options are available to full shell mirrors. We shall examine the Con-X alignment error budget and then describe each approach in turn, exploring their limitations with respect to focus error and imaging resolution.

2.1. Focus error sources and sensitivities

There are basically four sources of focus error for thermally formed mirror segments; cone angle errors in the mirror segments, radius (size) errors in the segments, axial position error of an otherwise aligned pair of segments, and axial spacing (despace) error of the secondary mirror relative to the primary. The focus error sensitivities can be calculated explicitly or determined via raytracing. These are shown for the 1.3 m SXT design for cone angle error and average radius error in Tables 1 and 2, respectively. We see that focus error is nearly two orders of magnitude more sensitive to cone angle error than to average radius error. This becomes an important issue later when we want to correct focus error.

Outermost Shell Focus Error (mm)					Innermost Shell Focus Error (mm)				
Primary Δr (um)	Secondary Δr (um)	+1	0	-1	Primary Δr (um)	Secondary Δr (um)	+1	0	-1
+1		+0.02	+1.54	+3.08	+1		+0.08	+6.65	+13.23
0		-1.52	0.0	+1.52	0		-6.57	0.0	+6.57
-1		-3.06	-1.54	-0.02	-1			-6.65	

Table 1: Axial focus error as a function of primary and secondary mirror cone angle errors for the 1.3m diameter design Con-X SXT. In the table cone angle error is expressed as delta-radius error, or Δr. This is the difference between the mirror radii at the large and small ends relative to the nominal design. Delta-radius divided by the mirror length (200 mm) yields the cone angle error.

Outermost Shell Focus Error (mm)					Innermost Shell Focus Error (mm)				
Primary avg. rad. (um)	Secondary avg. rad. (um)	+50	0	-50	Primary avg.rad. (um)	Secondary avg. rad. (um)	+50	0	-50
+50		+0.77	-0.38	-1.53	+50		+3.32	-1.65	-6.00
0		+1.15	0.0	-1.15	0		+4.97	0.0	-4.97
-50			+0.38	-0.77	-50			+1.65	-3.32

Table 2: Axial focus error as a function of primary and secondary mirror average radius errors for the 1.3m diameter design Con-X SXT.

With a fixed focal plane, we are concerned with the transverse aberration due to focus (spreading of the image on the detector), as this degrades imaging resolution. Because the entrance aperture of each shell is a narrow annulus (the radial width of the annuli range from approximately 3.25 to 0.75 mm for the 1.3 m diameter telescope design), focus error results in a ring shaped image from a full shell mirror, and an arc shaped image from Con-X mirror segments. By examination of the schematic image in Figure 3, we see that the linear radius of the ring or arc is given by:

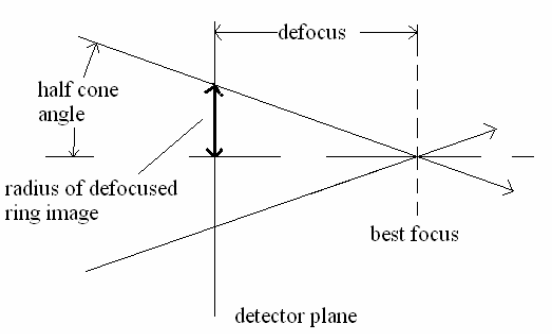

Figure 3: Schematic of focus error from a primary-secondary mirror pair. The converging cone of light from a single mirror shell is shown.

$$\delta r_F = \delta F \cdot \tan(\theta_C) = \delta F \cdot \tan(4\alpha) \qquad (1),$$

where θ_c is the half cone angle of the converging beam of light, $\alpha$is the graze angle at the intersection of primary and secondary mirrors, δF is the axial defocus, and δr_F is the radius of the arc formed by the defocused segment.

Despace between the secondary and primary mirror also produces defocus. 1 mm of despace produces 1.24 mm of defocus. Finally, if both primary and secondary mirrors are positioned incorrect axially, there is 1 mm of focus error per mm of axial position error (this is not strictly a focus error, but the effect is equivalent). Both of these errors are independent of the shell cone angle.

From Figures.3 and 4 we see that the arc of the defocused image at the detector plane has the same angular span as the does the mirror segment. In addition, if the focal length is too long (best focus is behind the detector) the arc image is on the same side of the optical axis as is the mirror segment. If the focal length is too short (best focus is between the mirror and the detector), than the arc image is on the opposite side of the optical axis from the mirror segment, and each point on the image is diametrically opposed to the corresponding point in the entrance aperture. Moreover, we also see that as we move (e.g.) clockwise around the mirror aperture, we also move in the same angular direction (i.e., clockwise) on the focal plane.

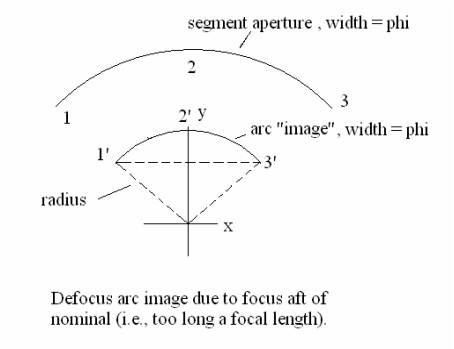

Figure 4: Projection of mirror segment aperture on focal plane with transverse focus error.

Sources of despace and axial positioning errors range from straightforward mirror positioning errors during alignment to the more subtle errors of selecting the wrong axial region of the oversized thermally formed mirror, or a prescription error in the thermal forming mandrel. (Mirrors are formed oversized and cut to proper size/shape after forming[4]). Sources of cone angle and radius errors include the mandrel figure, thermal forming related errors, and potential deformations introduced during mirror mounting.

Knowing the shape of the transverse aberration (Figure 4), the radius of the aberration (Figure 3 and eq. [1]), and the azimuthal span of the mirror segment, one can calculate either the rms or HPD image sizes. For the outermost shell, the image rms diameter as a function of defocus is ~ 0.5 arc-sec per mm defocus, for a 36 degree wide segment. For the innermost shell with a 72 degree span, the rms image diameter is ~ 0.22 arc-sec per mm defocus (the error does not scale linearly with cone angle as expected because the angular span of the segment has also doubled). The image HPD errors are ~ 0.42 and 0.19 arc-sec HPD per mm focus error, for the outermost and innermost mirror segments, respectively.

2.2. Alignment error budget

Error budgets have been developed for both 5 arc-sec and 15 arc-sec image half power diameter (HPD) resolution. These budgets, "living" documents as are all error budgets, were originally developed by Podgorski et al.[5] and have been modified and updated as the Con-X program has changed and advanced. The 5 arc-sec imaging HPD budget is summarized in the barely legible Figure 5. The pertinent contributors relative to mirror segment alignment are the terms representing 'focus and coma alignment' (item 30) – 0.71 arc-sec HPD, and 'reflector installation in module' (item 31) – 1 arc-sec HPD. The first term represents the post-alignment residual focus and coma errors relative to nominal. The second term represents the figure error and focus error introduced in a P-S pair of mirror segments as they are mounted in the module; i.e., this includes the effects of any mirror distortions purposely or accidentally introduced by final mounting. From the sensitivities in the previous section, the budget contribution, if due solely to focus error, limits the allowable focus error to less than +/- 1.7 mm for an outermost segment pair, and +/- 3.7 mm for an innermost segment pair. Of course, since there will be some residual coma error, in practice the maximum allowable focus error will need to be somewhat less than these values. (Note, any on-orbit average focus error of the entire mirror assembly can be corrected via a focal plane focusing mechanism).

2.3. Focus error correction by cone angle change

One approach to removing out-of-tolerance focus error contributors described in Section 2.1 is to change the cone angle of one or both mirrors of a P-S pair. As we have already seen in Section 2.1, focus is most sensitive to change in cone angle, thus, this is the parameter that gives us the greatest leverage in driving focus error down to an acceptable level. One of the advantages (and disadvantages) of thin, flexible, mirror segments is that they deform relatively easily. A mirror alignment and mounting system is being developed[5] that makes use of 5 mirror supports at each of the forward (large) and aft (small) ends of each mirror. These supports are radially adjustable during the alignment step of mounting a mirror segment. Utilizing an annular Hartmann test[6] such as was employed to align the Chandra X-ray Observatory mirrors to a fraction of an arc-second, the adjusters can be re-positioned so as to control mirror tip (pitch), and the radius of the forward and aft ends (segment tip, or yaw, is controlled by a separate set of adjusters). When satisfactory alignment is achieved, the mirror segment supports are bonded in place to the module housing and the adjuster mechanism removed.

The impact of such a system has been modeled using finite element techniques[7]. Development and testing of this system, specifically for its ability to change focal length via changing cone angle while introducing acceptably small local figure errors, is underway as part of the Con-X program. Results of this testing to date are reported on in this conference proceedings[8]. Modeling in reference 7 showed that up to 30 arc-sec of cone angle error can be corrected for each mirror segment with the introduction of 0.13 arc-sec RMS axial figure slope error. For two mirror surfaces this is equal to approximately 0.5 arc-sec HPD – one-half the error budget allocation of 1 arc-sec discussed in Section 2.2.

Using the focus error sensitivities to cone angle shown in Table 1, and the roughly 1:1 equivalence of a 1 arc-sec cone angle and a 1 um delta-radius error over a 200 mm long optic, we see that worst case correcting +/- 30 arc-sec cone angle error for each of the primary and secondary segments corresponds to correcting ~ 90 mm focus error for the outermost shell to ~ 400 mm focus error for the innermost shell. This means that this approach is useful for correcting focus errors that are out of tolerance (per the error budget allocation) by a factor of 50 to 100 – a very large acceptance range.

2.3. Focus error correction by coma compensation

An alternative alignment approach entails tilting the secondary mirror relative to the primary mirror to correct focus. Not really a focus correction approach, this method introduces comatic aberration (coma) to compensate for the transverse aberration due to focus error. We describe how this approach works. Coma is introduced by a relative tilt or decenter (a translation orthogonal to the optical axis) between the primary and

	ITEM (HPD - arcsec)	RQMT	Margin		Allocation					
1	Calorimeter Resolution	5.00	0.62							
2	On-Orbit Single Telescope			4.96						
3	Calorimeter pixelization error				0.96					
4	Telescope level effects				1.51					
5	Image Reconstruction errors (over obs)					1.41				
6	Attitude knowledge drift						1.00			
7	FMA/XMS focal plane drift (thermal)						1.00			
8	FMA/XMS vibration effects					0.20				
9	FMA/XMS misalignment (off-axis error)					0.05				
10	FMA/XMS Focus Error					0.50				
11	FMA On-orbit performance				4.63					
12	SXT Mirror launch shifts					0.50				
13	On-orbit Thermally Driven Errors					1.41				
14	Bulk temperature effects						1.00			
15	Gradient effects						1.00			
16	Material Stability					1.00				
17	FMA/Telescope mounting strain					1.00				
18	FMA, As built					4.14				
19	Gravity Release						1.00			
20	Bonding Strain						1.00			
21	Module to Module alignment						1.00			
22	Module						3.76			
23	Distort. & misalign due to module packing							0.71		
24	Mirror Pair Co-alignment							0.71		
25	Mirror Pair							3.63		
26	P-S alignment in module(using CDA)								1.12	
27	CDA Dynamic Accuracy									0.50
28	CDA Static Static Accuracy									0.50
29	Thermal Drift									0.50
30	Focus and Coma Alignment									0.71
31	Reflector Installation in module								1.00	
32	Reflector Pair (P-S)								3.30	
	Color Code	Rqmt		Margin	RSS Predict				Allocation	

Figure 5: 5 arc-sec imaging error budget for Con-X with a single SXT.

secondary mirrors. Like focus, because of the thin annular aperture nature of each shell of a Wolter I telescope, the transverse aberration due to coma is also a ring, or arc. But there are differences with focus. The focus arc has the same angular span as the mirror segment, and the center of the ring is the optical axis. Neither of these are the case for grazing incidence telescopes.

As shown in Figure 6, coma produces an arc-shaped image also, but the angular span of the arc is twice the angular span of the mirror segment. And the center of the comatic ring is displaced from the optical axis by a distance equal to the radius of the ring. Essentially (for the non-optical scientists), light incident at the top of the mirror segment (position '2' in the figure) and diametrically opposed (for a full shell mirror) are deviated the most, intersecting the focal plane at position '2 double prime' in the figure. Light that intersects the mirror along the +/- x axis in the figure ends up essentially undeviated, and intersects the focal plane at the optical axis. Thus, as we move around the entrance aperture for a full shell mirror, the comatically aberrated light from the telescope with describe two full circles on the focal plane (overlaying one another).

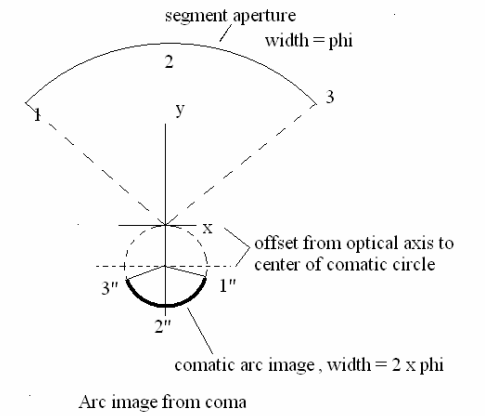

Figure 6: Schematic view of comatic aberration.

Thus, by introducing an amount of coma in the appropriate direction and with the diameter of the comatic circle approximately equal to the radius of the focus ring, it is possible to partially compensate for the transverse focus error. This can be seen in a spot diagram, shown in Figures 7a-d. In Figure 7a, the spot diagram shows the arc-like image from 2 arc-sec radius of focus. In Figure 7b is the spot diagram from 1 arc-sec radius of coma,

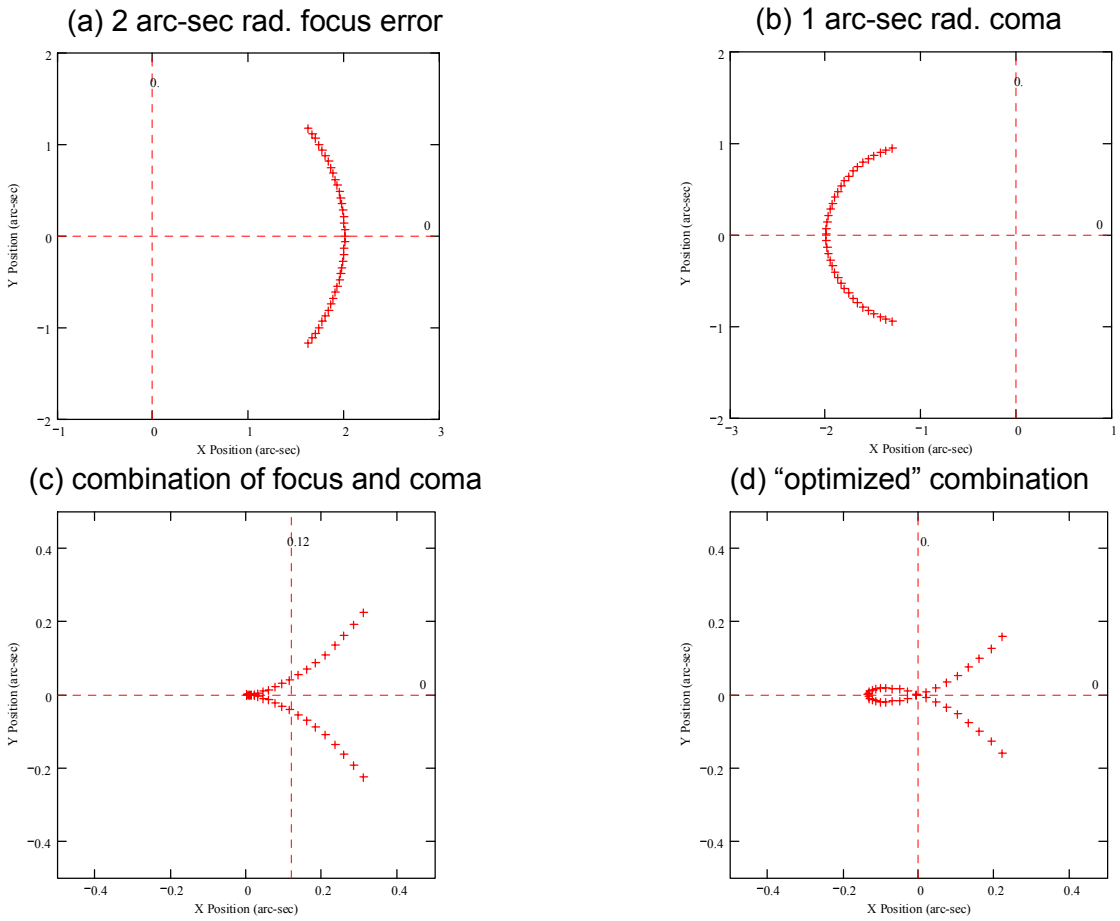

Figure 7: Spot diagrams of focus, coma, and coma compensated focus error for a 72 deg angular span Con-X P-S segment pair.

where the direction (sign) of the coma is chosen so as to lie on the opposite side of the optical axis from the focus 'arc'. (Basically, if the focus arc corresponds to too long a focal length, then the mirror segment is also to the right of the optical axis in fig. 7a, and we would adjust the secondary mirror such that its small end – closer to the focus – pitches towards the optical axis by an angle equal to the desired coma radius – 1 arc-sec). Figure 7c shows the spot diagram of the combination of the focus and coma errors. We see that the full Y axis span of the image has decreased from a little more than 2 arc-sec to ~ 0.5 arc-sec, and the full X axis span of the image has decreased from ~ 0.4 arc-sec to a little more than 0.3 arc-sec. In fact, we can optimize the amount of coma we add to the image to result in slightly better compensation than using the simple 2:1 rule, and this is shown in Figure 7d. Here, ~ 1.07 arc-sec of coma was added to the image rather than the 1 arc-sec in Fig. 7c.

Examining how the coma error compensates for the focus error will enable us to better understand the limitations of such an approach. The X and Y coordinates of the spots on the focal plane for a defocused image can be expressed as functions of the azimuthal position in the entrance aperture ϕ:

$$IX_{focus}(\phi) = A \cdot \cos(\phi) \qquad (2a),$$

and

$$IY_{focus}(\phi) = A \cdot \sin(\phi) \qquad (2b),$$

where A is the radius of the transverse focus aberration and can be positive or negative depending upon whether the focal length is too long or too short. Similarly, for an image with coma,

$$IX_{coma}(\phi) = B \cdot \cos(2 \cdot \phi + \phi_{coma}) + B \cdot \cos(\phi_{coma}) \quad (3a),$$

and

$$IY_{coma}(\phi) = B \cdot \sin(2 \cdot \phi + \phi_{coma}) + B \cdot \sin(\phi_{coma}) \quad (3b),$$

where B is the radius of the coma aberration and ϕ_{coma} is the phase of the coma. From the equations we see the coma dependence upon twice the azimuthal position in the entrance aperture. The chord of the focus arc is represented as:

$$\Delta y_{focus} = 2 \cdot \delta r_F \cdot \sin(\phi/2) \quad (4).$$

The chord of the compensating coma error is expressed as:

$$\Delta y_{coma} = 2 \cdot \frac{\delta r_F}{2} \cdot \sin(\phi) \quad (5).$$

Then, the relative residual $\Delta y_{resid}^{relative}$, after subtracting the comatic aberration from the focus aberration, or $(\Delta y_{focus} - \Delta y_{coma})/ \Delta y_{focus} = 1 - \Delta y_{coma}/ \Delta y_{focus}$, may be written as:

$$\Delta y_{resid}^{relative} = 1 - \frac{\sin(\phi)}{2 \cdot \sin(\phi/2)} \quad (6).$$

Clearly, only for segment azimuthal spans ϕ over which the sine function is very nearly linear is the compensation very good; the larger ϕ, the poorer the compensation. As examples, for $\phi = 36$ degrees, the relative residual chord error is 0.049. But for $\phi = 72$ degrees, the relative residual chord error is 0.19, nearly four times larger – the degree of coma compensation decreases approximately as the square of the azimuthal span of the mirror segment. Using an optimized value of coma only makes a small improvement to this.

Calculating the residual image size after coma compensation for the innermost, 72 degree span segment pair, and the outermost, 36 degree span segment pair, we find that:

a. a 36 degree segment pair has a residual of 0.052 arc-sec HPD per 1 arc-sec initial focus error radius, and

b. a 72 degree segment pair has a residual of 0.22 arc-sec HPD per 1 arc-sec initial focus error radius.

Limiting the focus contribution to imaging to the 0.7 arc-sec HPD in the error budget limits the focus error to +/- 11 mm for either the innermost segment pair or the outermost segment pair. If we consider that in practice there will be some residual coma error in the orthogonal direction, the allowable focus error tolerances will be somewhat smaller than the +/- 11 mm.

2.4. Comparison of the two focus error correction methods

Cone angle correction of focus error using an adjustable mirror mount allows for correction of focus errors between +/- 90 and +/- 400 mm, for outermost to innermost shells, respectively. Coma compensation of

focus error can be used for focal length errors of a P_S segment pair up to +/- 11 mm. For a 5 arc-sec imaging error budget, the focus error allocation is consistent with limiting focus error to +/- 1.7 to 3.7 mm (outermost to innermost shells).

Based upon the acceptable focus error tolerances for the two techniques of correcting focus, the cone angle adjustment method has a significantly greater tolerance band and is therefore the more advantageous method if large focus errors are present. The coma compensation approach, on the other hand, requires less complex adjustment – only a rigid body tilt of the secondary mirror – and so is simpler and easier to effect than the cone angle adjustment. Thus, the real trade as to which approach is used to correct focus errors is really determined by the focus error tolerance of the as-fabricated mirror segments. Given the present uncertainties regarding focal length errors at this point of the Constellation-X program, we are currently pursuing both the active cone angle adjustment and the simpler coma compensation methods.

3. SUMMARY

The Con-X Observatory will contain one or four Spectroscopy X–ray Telescopes which are comprised of many pairs of primary and secondary mirror segments. To meet imaging resolution requirements and error budgets, it is necessary that each segment pair be made to focus at the same point on the focal plane within a small axial tolerance. In order to make the mirror pairs confocal, two alignment techniques have been identified and are being studied. In one case, the cone angle of the individual mirror segments is adjusted by a set of 5 radial adjusters at each of the small and large ends of the segments. This approach offers the broadest focus error tolerance band that can be satisfactorily corrected while still meeting imaging resolution error budgets. The second technique, coma compensation of focus error makes use of adding in comatic aberration via tilting the secondary mirror relative to the primary. It results in compensation of the transverse aberration from focus, improving (reducing) the image core. This method has a much smaller range of correction than the cone angle adjustment method, but it is also much simpler to accomplish.

4. ACKNOWLEDGEMENTS

This work was supported under NASA Contract NNX08AB46A. The authors also thank Paul Glenn and Timo Saha for many useful discussion.

5. REFERENCES

1. N.E. White and H. Tananbaum, “Constellation-X Mission: Science Objectives and implementation Plan”, SPIE Proc., vol. **4851**, 293 (2003).

2. R. Petre, *et al.*, “Constellation-X Spectroscopy X-ray Telescope (SXT)”, SPIE Proc., vol. **4851**, 433 (2003).

3. Zhang, W. W.; Bolognese, J.; Chan, K. W.; Content, D. A.; Hadjimichael, T. J.; He, Charles; Hong, M.; Lehan, J. P.; Mazzarella, J. M.; Nguyen, D. T.; Olsen, L.; Owens, S. M.; Petre, R.; Saha, T. T.; Sharpe, M.; Sturm, J.; Wallace, T.; Gubarev, M. V.; Jones, W. D.; O'Dell, S. L.; Davis, W.; Freeman, M.; Podgorski, W.; Reid, P. B. “Constellation-X mirror technology development,” SPIE Proc., vol. **6686**, 1 (2007) .

4. William Zhang, David Content, Stephen Henderson, John Lehan, Robert Petre, Timo Saha, Stephen O’Dell, William Jones, William Podgorski, and Paul Reid, “Development of Lightweight X-Ray Mirrors for the Constellation-X Mission”, SPIE Proc. **5488**, 820 (2004).

5. William A. Podgorski, Jay Bookbinder, David A. Content, William N. Davis, Mark D. Freeman, Jason H. Hair, Scott M. Owens, Robert Petre, Paul Reid, Timo T. Saha, Jeffrey W. Stewart, and William W. Zhang, "Constellation-X spectroscopy x-ray telescope optical assembly pathfinder image error budget and performance prediction", SPIE Proc., **5168**, 318 (2004).

6. Paul Glenn, "Centroid detector assembly for the AXAF-I alignment test system," SPIE Proc., vol. **2515**, 352 (1995).

7. William Podgorski and William Davis, "Radius, Cone Angle and Optic Installation(into Housing) Tolerances," Smithsonian Astrophysical Observatory Internal Memorandum, 16 May 2003.

8. William Podgorski, David Caldwell, William Davis, Mark Freeman, Scott Owens, Paul Reid, and William Zhang, "A mounting and alignment approach for Constellation-X mirror segments," SPIE Proc., *to be published this proceedings*.